Int. J. of Applied Mechanics and Engineering, 2006, vol.11, No.1, pp.123-141

NETWORK THEORY OF ELECTRO-RHEOLOGICAL FLUID AND ITS HYDRODYNAMIC CHARACTERISTICS IN A PARALLEL DUCT

K. SHIMADA*
Fukushima University, 1 Kanayagawa
Fukushima, 960-1296, JAPAN
e-mail: l10ol1@sss.fukushima-u.ac.jp

T. TATEISHI
School of Engineering, University of Southern California
Los Angeles, CA 90089-0241, USA

H. YAMAGUCHI
Doshisya University, 1-3 Tatara-tsugaya
Kyotanabe, 610-0321, JAPAN

We proposed a shear rheological relation based on a network theory regarding a suspension-type electro-rheological fluid (ERF) containing smectite particles. The theoretical constitutive equations concerning ERF under a D. C. electric field were derived using Rodge's network theory. The equations have creative and destructive functions expressing behavior as aggregated particles influenced by shear flow and an electric field. The theoretical results regarding viscosity based on the theoretical equations were compared with experimental data concerning the static shear stress in relation to shear rate obtained using a rotating concentric cylindrical rheometer. The viscosity behaves as a non-affine motion at a small shear rate range and as affine motion at large one. We investigated the parameters in the equations of the network theory. Next, we applied the proposed network theory to a rectangular duct ERF flow problem. The theoretical result can explain quantitatively the experimental data regarding pressure difference at a large given flow velocity. At a small given flow velocity range, the mechanical model containing the Maxwell model by Shimada can explain the experimental data quantitatively.

Key words: electro-rheological fluid, network theory, electric field, viscosity, flow, non-affine motion, affine motion, mechanical model.

* To whom correspondence should be addressed

1. Introduction

ERF is a functional or intelligent fluid reacted upon by an electric field. Based on the characteristics of the fluid's electric reaction, many engineering applications have been proposed including use in a braking device by Shimada and Fujita (2000b), damper by Gavin *et al.* (1996), Stanway *et al.* (1996b), Wereley and Pang (1998), Lee *et al.* (2002), and Lindler and Wereley (2003), clutch by Johnson *et al.* (1993), Whittle *et al.* (1995), Peel *et al*. (1996), and Oravsky (2002), etc.. As for more development of their applications, a theoretical investigation from the point of view of hydrodynamics is needed. However, a few theoretical investigations of ERF's hydrodynamic characteristics have been performed, especially with regard to various flow fields (Zkakin and Tarapov, 1979; Gogosov *et al.*, 1979; Prudnikov, 1979; ARP *et al.*, 1980; Sasada and Honda, 1980; Klingenberg *et al.*, 1991; Atkin *et al.*, 1991 and Brunn and Abu-Jdayil, 1998). There is one method in order to understand and clarify the inner physical ERF's characteristics in the hydrodynamic investigations: lumped parameter or mechanisms-based model utilizing a dynamic mechanical model of ERF by Stanway *et al.* (1987a), Gamota and Filisko (1991), and Kamath and Wereley (1997). To date Shimada *et al*. (2000c) have also conducted numerical calculations regarding a rectangular duct flow by using the proposed dynamic mechanical model of ERF.

By applying an electric field, particles of suspension-type ERF are known to aggregate as many chain-like clusters between electrodes (Halsey, 1992). Along the direction of the electric field line, the particles are bound by reciprocal forces among particles, for example, the forces of dipole moments of the particles, Van der Waals forces, etc.. These reciprocal forces have been investigated theoretically by Martin *et al*. (1996) in relation to the aggregated force of ERF. However, reciprocal forces also exist between these chains as seen by Martin and Anderson (1996) and Yang (1997). Therefore, it should be considered that in every coordinate direction, particles are bound by reciprocal forces. This behavior is similar to that of a network and the result enables a network theory to be derived in regard to ERF.

As well, the actual presence of a network can be confirmed in ERF. Initially, we confirm this under an electric field in the case of ERF that contains micro-meter sized whisker particles. Many junctions in ERF having needle-like whisker particles can be observed microscopically under an electric field as shown in Fig.1 in **APPENDIX A**.

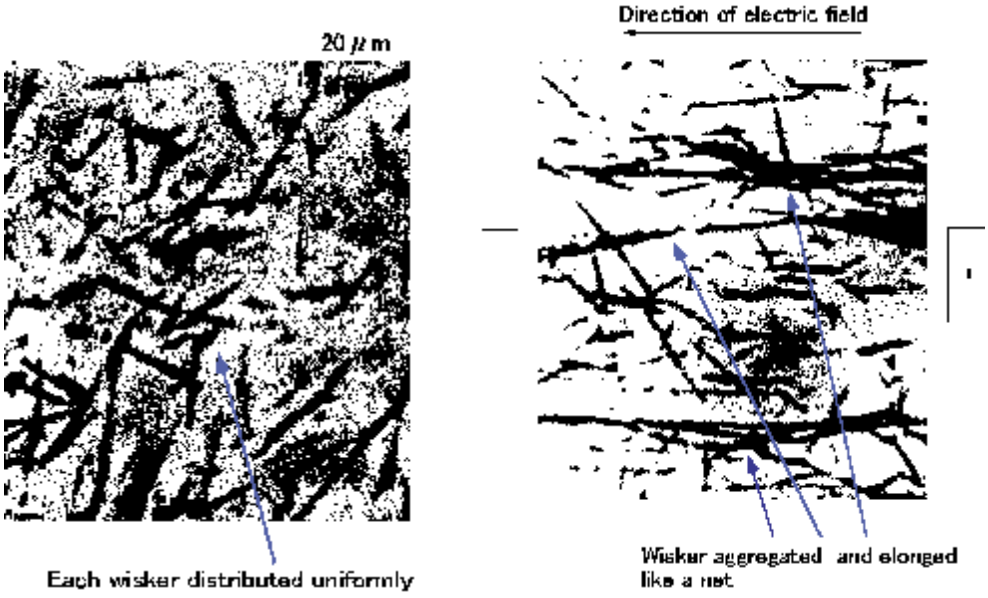

a) Under no applying an electric field. b) Under a D.C. electric field.

Fig.1. Photograph of ERF containing whisker particles between electrodes.

The relation between shear rate and shear stress of the ERF having the whisker particles is shown in Fig.2. In another investigation, we can obtain the experimental result that storage and loss moduli G' and G'' of an ERF having smectite particles in both cases with and without an electric field are greater than those of normal polymeric suspension as shown in Fig.3 in **APPENDIX B**. In the present study, an ERF having smectite particles is dealt with as an ERF used in order to validate our proposed network theory in the light of experimental data. In the case of ERF having another type of particles, the G' and G'' of an ERF have been investigated by Otsubo *et al*. (1997) and Kim *et al.* (1999).

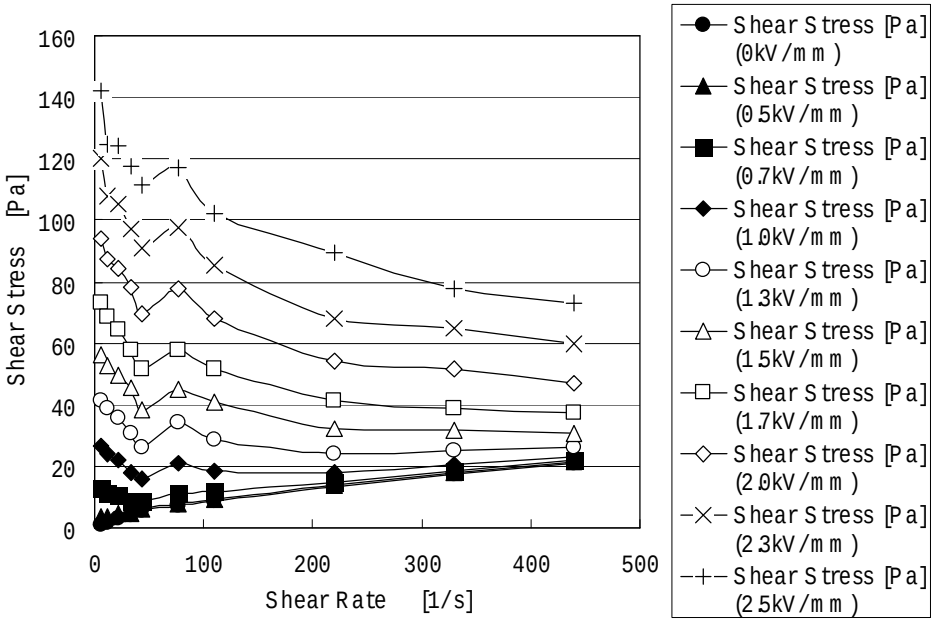

Fig.2. Shear stress to shear rate of ERF containing whisker particles.

a)

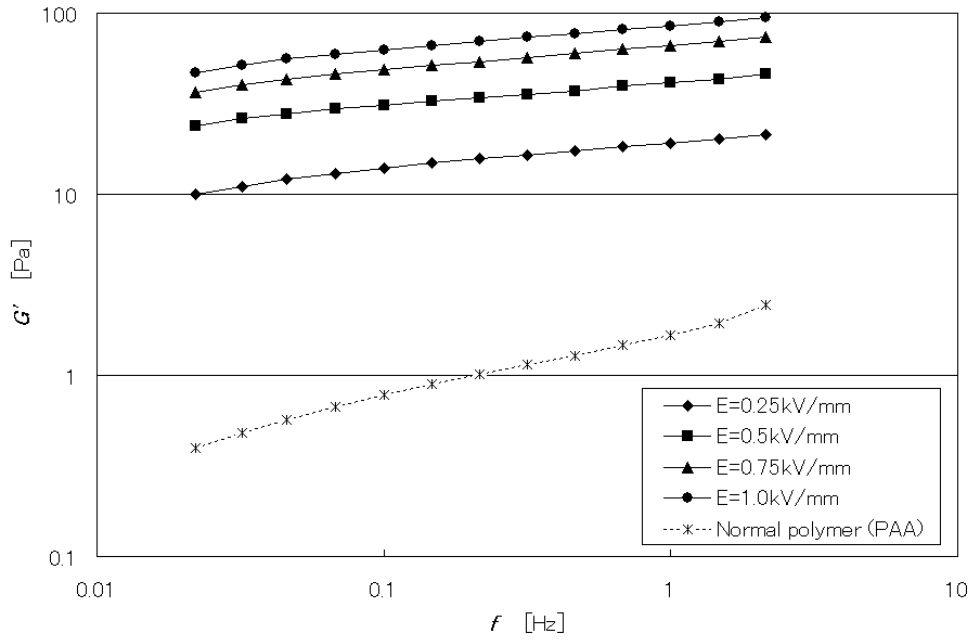

b)

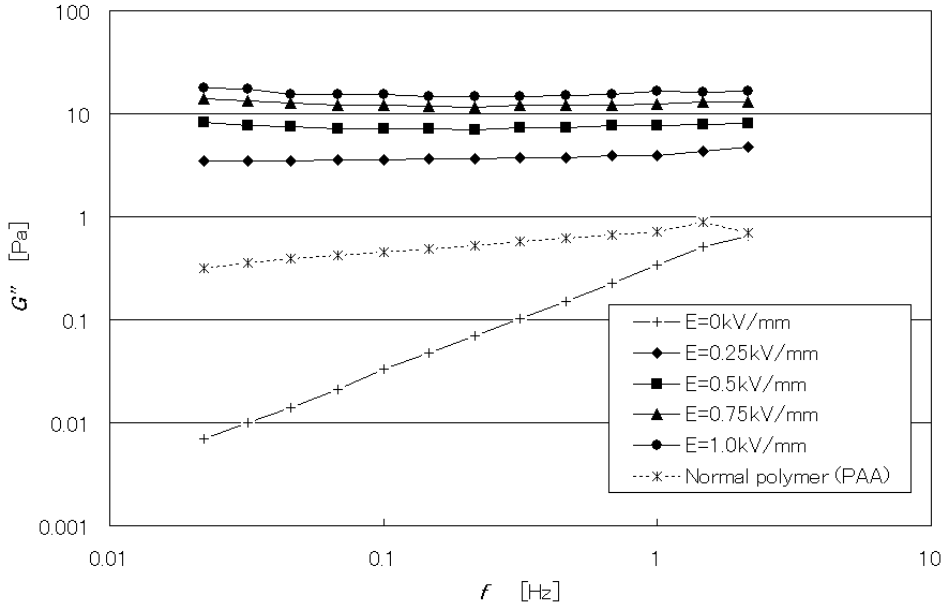

Fig.3. Experimental data of G' and G'' of ERF containing smectite particles compared with the ones of polyacrylicamide (PAA) as a normal polymer.

Based on the above results, a network theory can be derived regarding ERF. However, a theory or theoretical model treating ERF as a network has not been proposed in the literature until recently. The network theory of ERF provides one explanation of the rheological characteristics of ERF by means of constitutive equations and can be expected to allow an analysis of the motion of ERF in regard to its theoretical hydrodynamics. The network theory has not been applied to certain ERF flow problems.

On the other hand, the rheological and electric characteristics regarding viscosity, electric current, and so on in a rotating flow of ERF containing smectite particles has been investigated by Shimada *et al.* (2000d), Nishida *et al.* (1999a), Nishida *et al.* (1999b), Nishida *et al.* (1999c), and Nishida *et al.* (2002d). This same ERF was also applied to a rotating device regarding braking device, rotating regulator, etc., and the static and dynamic characteristics were investigated by Shimada and Fujita (2000b) and Nishida and Shimada (2002e). This ERF does not have the same high yield stress and shear stress at a large shear rate as the ordinary ERF utilized in many engineering applications. However, the ERF containing the smectite

particles is suitable for engineering applications because particles do not stratify or settle easily during the static state for a long time. In general, this is a very important necessary condition in the field of ERF. Therefore, it is valuable to utilize the ERF containing smectite particles as a model ERF in the engineering application, and to investigate the characteristics of this ERF and of devices utilizing this ERF.

In the present paper, therefore, we propose a network theory of a suspension-type ERF using hydrodynamic constitutive equations. In the derivation, Rodge's Network Model by Bird *et al.* (1987) is used. Next, we deal with the ERF containing smectite particles. The theoretical results are compared with experimental data of viscosity. In addition, we deal with a rectangular duct ERF flow problem as an ERF flow in order to investigate the possibility of the usage of the theory in any ERF flow problems, and apply the proposed ERF network theory to the rectangular duct ERF flow.

2. Network theory

2.1. Distribution function

When no electric field is applied to ERF, the spherical particles are distributed uniformly in a solvent. By applying an electric field, a dipole moment occurs in each particle. Due to the electric correlations among particles that then occur among the dipole moments, the particles are thought to be structured like a network with junctions. As shown in Fig.4, the particles are pointed toward the junctions, and the segments, as chains between the junctions, are composed of parts of particles. The end-to-end junction vector for a typical segment is given by $\boldsymbol{Q}$. The network theory is based on six common assumptions for both solids and liquids, as described by Bird *et al.* (1987); for example, the network junction points move as an affine motion: each network segment can be modeled as a Gaussian chain. The number density of $\boldsymbol{Q}$ existing between $\boldsymbol{Q}$ and $\boldsymbol{Q}+d\boldsymbol{Q}$ is shown by Eq.(2.1).

$$n(t)\varphi(\boldsymbol{Q},t)d\boldsymbol{Q} \tag{2.1}$$

where $n(t)$ is the number density, t the time, and $\varphi(\boldsymbol{Q},t)$ the probability density function.

The distribution function $\Psi(\boldsymbol{Q},t)$ is defined by Eq.(2.2)

$$\Psi(\boldsymbol{Q},t)d\boldsymbol{Q} \equiv n(t)\varphi(\boldsymbol{Q},t)d\boldsymbol{Q}\,. \tag{2.2}$$

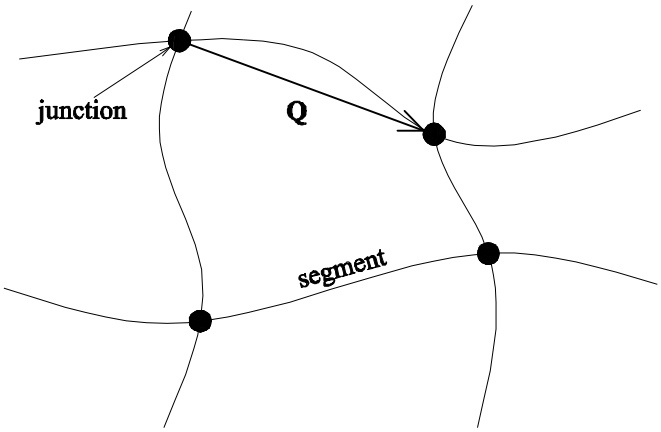

Fig.4. Schematic diagram of ERF network and end to end vector. The particles are located at the junction.

2.2. Liouville equation

The equation of continuity for $\Psi(\boldsymbol{Q},t)$ is given as Eq.(2.3) by R. Huilgol and Phan-Thien (1997)

$$\frac{\partial\Psi(\boldsymbol{Q},t)}{\partial t}=-\frac{\partial}{\partial\boldsymbol{Q}}\cdot\left(\dot{\boldsymbol{Q}}\Psi(\boldsymbol{Q},t)\right)+L(Q,t)-\frac{\Psi(\boldsymbol{Q},t)}{\lambda(Q,t)} \tag{2.3}$$

where $L(Q,t)$ is the creative function, $\lambda(\boldsymbol{Q},t)$ the destruction function, and $\dot{\boldsymbol{Q}}$ the velocity of end-to-end vector $\boldsymbol{Q}$ as shown by Eq.(2.4)

$$\dot{\boldsymbol{Q}}=(\nabla\upsilon)^{t}\cdot\boldsymbol{Q} \tag{2.4}$$

where $\boldsymbol{v}$ is the velocity of solvent.

2.3. Creative function

The creative function $L(Q,t)$ in Eq.(2.3) represents the increasing amount of $n(t)$ per unit time and can be represented by using the probability density function φ_{eq} and the creative ratio of the network per unit time *f*.

$$L(Q,t)=f\ \varphi_{eq}. \tag{2.5}$$

In the present study, we define $L(Q,t)$ taking into account the relation between the electric field

strength and the ratio of the completion of the created network as well as the relation between the magnitude of the shear rate and the ratio of the completion of the created network. Initially, we consider the commonly known facts about ERF: the transit time from application of an electric field to completion of the created network decreases as the electric field strength increases: the order of the transit time, as the response time from the applied field, R is approximately a millisecond. For example, Tanaka *et al.* (1995) demonstrated that there is little difference in $L(Q,t)$ with regard to the electric field strength E in the range of large E, and the effect of E on $L(Q,t)$ is large in the range of small E. Therefore, f which means the relation between the shear rate intensity and the creative ratio of the network can be given by the exponential function as in Eq.(2.6)

$$f = 1 - \exp\left(-\theta\frac{E}{R}\right) \tag{2.6}$$

where θ is the constant.

Secondly, based on the response time of the network to the shear flow being much less than the relaxation time induced by the shear stress, the effect of the shear rate on the creative function can be ignored. Therefore, it is assumed that the creative function is in a quasi-equilibrium state. The probability density function φ_{eq} in the quasi-equilibrium state can then be formulated by the Gaussian distribution, as shown in Eq.(2.7)

$$\varphi_{eq}(Q) = \left(\frac{H}{2\pi kT}\right)^{3/2}\exp\left(-\frac{H}{2kT}\right)Q^2 \tag{2.7}$$

where H is the spring constant of a segment between the particles, k the Boltsmann constant, and T the absolute temperature.

Based on the above, the creative function $L(Q,t)$ can be defined as shown by Eq.(2.8)

$$L(Q,E) - \hat{L}\left(1 - e^{-\theta\frac{E}{R}}\right)\varphi_{eq}(\boldsymbol{Q}) \tag{2.8}$$

where $\hat{L}$ is a constant.

2.4. Destruction function

Destruction of the network can be thought to be a result of shear flow and Brownian motion. At a small shear rate, the effect of shear flow on the network destruction is small, because particles aggregate easily under an electric field. However, the probability of destruction increases at a large shear rate, as this destruction depends primarily on the effects of the shear flow. Therefore, the destruction function $\lambda(Q,t)$ is defined as a function of the shear rate and as the probability per unit time, as shown by Eq.(2.9)

$$\frac{1}{\lambda(\dot{\gamma})} = 1 - \exp\left(-\frac{\dot{\gamma}+b}{\mu}\right)^{n_o} \tag{2.9}$$

where n_o, μ and b are constants, and $\dot{\gamma}$ is the magnitude of the shear rate intensity.

2.5. Liouville equation of ERF

When the Liouville equation, as shown by Eq.(2.3), is applied to ERF, Eq.(2.10) can be given as

$$\frac{\partial \Psi(\boldsymbol{Q},t)}{\partial t} = -\frac{\partial}{\partial \boldsymbol{Q}} \cdot (\boldsymbol{Q}\Psi(\boldsymbol{Q},t)) + L(Q,E) - \frac{\Psi(\boldsymbol{Q},t)}{\lambda(\dot{\gamma})}. \tag{2.10}$$

By substituting Eq.(2.4) into Eq.(2.10), multiplying Eq.(2.10) by $\boldsymbol{QQ}$, and integrating Eq.(2.10) at all areas of the arranged space for the network, Eq.(2.11), using $\langle \boldsymbol{QQ} \rangle_N$ as the mean value of $\boldsymbol{QQ}$, can be given as

$$\frac{\partial \langle \boldsymbol{QQ} \rangle_N}{\partial t} = \left\{ (\nabla \upsilon) \cdot \langle \boldsymbol{QQ} \rangle_N + \langle \boldsymbol{QQ} \rangle_N \cdot (\nabla \upsilon)^t \right\} = \zeta \underset{\approx}{\delta} - \frac{\langle \boldsymbol{QQ} \rangle_N}{\lambda(\dot{\gamma})} \tag{2.11}$$

where ζ is the function related to the creation of the network, as shown by Eq.(2.12), a the particle radius, and $\underset{\approx}{\delta}$ the Kronecker's delta. In the present study, the arrangement of particles is assumed to be a network. On the other hand, it is commonly known that, under an electric field, ERF particles are aggregated like many chains in a cluster. Therefore, N is the number of particles composing the chain

$$\zeta \equiv \frac{1}{3}\hat{L}\left(1 - e^{-\theta\frac{E}{R}}\right)(N-1)_a^2. \tag{2.12}$$

As $\langle \boldsymbol{QQ} \rangle_N$ is the function of time, $\boldsymbol{v} \cdot \langle \boldsymbol{QQ} \rangle_N = 0$. This relation is substituted into the left-hand side of Eq.(2.11), and Eq.(2.11) becomes Eq.(2.13)

$$\frac{D\langle \boldsymbol{QQ} \rangle_N}{Dt} - \left\{ (\nabla \upsilon) \cdot \langle \boldsymbol{QQ} \rangle_N + \langle \boldsymbol{QQ} \rangle_N \cdot (\nabla \upsilon)^t \right\} = \zeta \underset{\approx}{\delta} - \frac{\langle \boldsymbol{QQ} \rangle_N}{\lambda(\underset{\approx}{\dot{\gamma}})} . \tag{2.13}$$

As the left-hand of Eq.(2.13) is the upper convective derivative represented as ∇, it can also be represented by Eq.(2.14)

$$\left\langle \overset{\nabla}{\boldsymbol{QQ}} \right\rangle_N = \zeta \underset{\approx}{\delta} \frac{\langle \boldsymbol{QQ} \rangle_N}{\lambda(\underset{\approx}{\dot{\gamma}})} . \tag{2.14}$$

2.6. Shear stress tensor

All of the shear stress tensors in ERF $\underset{\approx}{p}$ can be represented as the sum of the shear stress tensor of solvent $\underset{\approx S}{p}$ and that of network $\underset{\approx N}{p}$

$$\underset{\approx}{p} = \underset{\approx S}{p} + \underset{\approx N}{p} . \tag{2.15}$$

$\underset{\approx S}{p}$ is represented as shown by Eq.(2.16) with P_S as the static pressure in the solvent and shear stress tensor in the solvent $\underset{\approx S}{t}$, η_S the viscosity of the solvent, and $\underset{\approx}{\dot{\gamma}}$ the shear rate tensor

$$\underset{\approx S}{p} = -P_S \underset{\approx}{\delta} + \underset{\approx S}{t} = -P_S \underset{\approx}{\delta} + \eta_S \underset{\approx}{\dot{\gamma}} . \tag{2.16}$$

$\underset{\approx N}{t}$ in Eq.(2.15) is represented by Eq.(2.17) using the tension $\boldsymbol{F}(E, \boldsymbol{Q})$ on a segment of the network

$$\underset{\approx N}{\mathrm{p}} = \langle \boldsymbol{QF} \rangle_N \tag{2.17}$$

where $\boldsymbol{F}(E, \boldsymbol{Q})$ assumes that the shear stress on a segment is equal to that on a Gaussian chain, and is defined by Eq.(2.18)

$$F(E, \boldsymbol{Q}) = \boldsymbol{H}_N(E)\boldsymbol{Q} \tag{2.18}$$

where $H_N(E)$ is the spring constant of a segment between the particles, which is a function of the electric field strength, and it is assumed to be represented by Eq.(2.19) under the assumption that the aggregated force along the direction of the electric line of force between particles in ERF is in proportion to the electric field strength as seen in Gast and Zukoski (1989) and Doi (1994)

$$H_N(E) = HE^M \tag{2.19}$$

where M are constants. H is assumed to have a proportional constant of $\varepsilon_o \beta^2 a^2$, where ε_o is the permittivity in a vacuum and β the specific permittivity.

Equation (2.18) becomes Eq.(2.20) using Eq.(2.19), as follows

$$F(E, \boldsymbol{Q}) = H_E^M \boldsymbol{Q}. \tag{2.20}$$

Equation (2.17) becomes Eq.(2.21) by substituting Eq.(2.20), as follows

$$\underset{\approx N}{\mathrm{p}} = H_N(E)\langle \boldsymbol{QQ} \rangle_N. \tag{2.21}$$

2.7. Constitutive equation

From Eqs (2.14) and (2.21), a form of the constitutive equation for the network can be obtained as follows

$$\underset{\approx N}{\mathrm{p}} + \lambda(\psi) \overset{\nabla}{\underset{\approx N}{\mathrm{p}}} = \lambda^2(\psi)\zeta H_N(E)\underset{\approx}{\delta} \tag{2.22}$$

where $\underset{\approx}{p}_N$ is represented by Eq.(2.23)

$$\underset{\approx}{p}_N = -P_N \underset{\approx}{\delta} + \underset{\approx}{t}_N \tag{2.23}$$

where P_N is the static pressure of the network.

On the other hand, a form of the stress tensor for the solvent is presented by Eq.(2.16). The total stress tensor is presented by Eq.(2.15). By substituting Eqs (2.23) and (2.16) into Eq.(2.15) with $P = P_N + P_S$ and $\underset{\approx}{p}_S = \eta_S \underset{\approx}{\dot{\gamma}}$, the final form of stress tensor is presented by Eq.(2.24) considering the condition of shear stress under the static condition represented as $\dot{\gamma} = 0$

$$\begin{aligned} &\underset{\approx}{p}_S = -P_S \underset{\approx}{\delta} + \eta_S \dot{\gamma} \underset{\approx}{\dot{\gamma}} + \underset{\approx}{t}_N, \\ &\underset{\approx}{t}_N + \lambda(\dot{\gamma}) \overset{\nabla}{\underset{\approx}{t}}_N = \lambda^2(\dot{\gamma}) \zeta H_N(E) \dot{\gamma}. \end{aligned} \tag{2.24}$$

2.8. Viscosity of affine motion

From Eq.(2.24), viscosity under the assumption of Couette flow is obtained as Eq.(2.25)

$$\eta = \eta_S + \lambda^2(\dot{\gamma}) \zeta H_N(E) \tag{2.25}$$

where the second part of the right hand is presented by Eq.(2.26)

$$\lambda^N(\dot{\gamma}) \zeta H_S(E) = \frac{\left\{ \frac{1}{3} \hat{L} \left(1 - e^{\left(-\theta \frac{E}{\mu} \right)} \right) (N-1) a^4 \varepsilon_o \beta^2 \right\} E^M}{\left(1 - \exp\left(\frac{\dot{\gamma} + b}{\mu} \right)^{n_o} \right)^2}. \tag{2.26}$$

2.9. Viscosity of non-affine motion

In the network theory, non-affine motion refers to the motion of the network, taking into consideration the difference between the velocities of the network and that of the solvent as seen in Bird *et al.* (1987). The equation of non-affine motion of ERF is represented as Eq.(2.27), using the slip parameter ξ as seen in Bird *et al.* (1987) and Huilgol and Phan-Thien (1997)

$$\overset{\nabla}{\boldsymbol{Q}} = (\nabla \cdot v)^t \cdot \boldsymbol{Q} - \frac{1}{2}\xi \underset{\approx}{\dot{\gamma}} \cdot \boldsymbol{Q}. \tag{2.27}$$

If the relative velocity between the solvent velocity and that of the network is zero, represented as $\xi = 0$, Eq.(2.27) coincides with Eq.(2.4). Using Eq.(2.27), the constitutive equation of ERF as non-affine motion can be derived as Eq.(2.28)

$$\underset{\approx N}{t} + \lambda(\dot{\gamma})\left\{ \overset{\nabla}{\underset{\approx N}{t}} + \frac{1}{2}\xi\left(\underset{\approx}{\dot{\gamma}} \cdot \underset{\approx N}{t} + \underset{\approx N}{t} \cdot \underset{\approx}{\dot{\gamma}} \right) \right\} = \lambda^2(\dot{\gamma})\zeta H_N(E)(1-\xi)\underset{\approx}{\dot{\gamma}}. \tag{2.28}$$

From Eq.(2.28), viscosity under the assumption of Couette flow is obtained as Eq.(2.29)

$$\eta = \eta_S + \frac{\zeta H_S(E)(1-\xi)}{1+\xi(2-\xi)\dot{\gamma}^2}. \tag{2.29}$$

3. Experimental procedure of viscosity

The ERF used in the present paper is a colloidal suspension containing smectite particles of $Na_{0,4}Mg_{2,6}Li_{0,4}Si_{4,0}O_{10}(OH)_{2,0}$ in a silicone oil with a mass concentration of *3.0 wt %*, that was developed by Fujita *et al.* (1997). The distribution of particles in the solvent of this ERF is very stable. The smectite particles are made up of some aluminosilicate layers of *10-100 nm* diameter. As a solvent flows between the layers, the smectite particle can be expanded. Therefore, the length of the smectite particle is *2-50 nm.*

The instrument used to measure the viscosity of the ERF was a concentric cylinder-type rheometer (RS75 by HAKKE Co. Ltd.) having a rotating inner cylinder of a diameter of *40 mm* and a static outer cylinder of a diameter of *42 mm*. An electric field is applied between the cylinders as $E = 1.00$, 1.50, 2.00 kV/mm by a high DC-voltage power supply. The temperature of the ERF was held constant at $20^0 C$. The experimental range of the shear rate was $0.02 - 10001/s$.

4. Viscosity of ERF

The viscosity of ERF having smectite particles at a shear rate range of $0.02-10001/s$ is determined by comparing the theoretical results obtained using Eq.(2.29) for non-affine motion and Eq.(2.25) for affine motion. In the case of affine motion, $M, n_o, \mu, b, \hat{L}, \theta$ and N are variable functions. In the case of non-affine motion, $M, n_o, \mu, b, \hat{L}, \theta, N, R$ and ξ are variable functions. In the case of affine motion, under the condition of $\eta_o = 0.020$, $a = 2.00\times10^{-9}$, $\varepsilon_S = 2$, $\varepsilon_p = 3$, $\varepsilon_o = 8.85\times10^{-12}$ and $\beta = 0.224$, we obtained the theoretical results in the case of $M = 1.25$, $n_o = 0.500$, $\mu = 1000.0$, $b = 0.1$, $\hat{L} = 1.00\times10^{36}$, $\theta = 1$, and $N=50$ by fitting the experimental data. In the case of non-affine motion, under the same condition of $\eta_o, a, \varepsilon_S, \varepsilon_p, \varepsilon_o$ and β, we obtained the theoretical results in the case of $M = 3.50$, $n_o = 0.750$, $\mu = 4000$, $b = 90.0$, $\hat{L} = 1.20\times10^{34}$, $\theta = 1$, $N = 50$, $R = 1.00$, and $\xi = 0.500$ by fitting the experimental data.

The theoretical results agree strongly with the experimental data regarding non-affine motion in a small shear rate range and with affine motion in a large one. In the range of the largest shear rate, the viscosity under the electric field approaches that without an electric field because at this range the particle networks have been destroyed and their distribution in the ERF becomes uniform. However, there is a region of quantitative discrepancy between the experimental and theoretical fitted results at medium shear rate range in Fig.5. The cause is dependent on the kind of ERF. Because we confirmed that the other ERFs except for the present ERF have quantitative coincidence or quantitative discrepancy at some shear rate. In the present study, since the behavior of the smectite particle induces the creation of the network as follows, the theoretical analysis at a flow in a rectangular duct is progressed as approving the quantitative difference between the experimental and theoretical fitted results at medium shear rate range.

a)

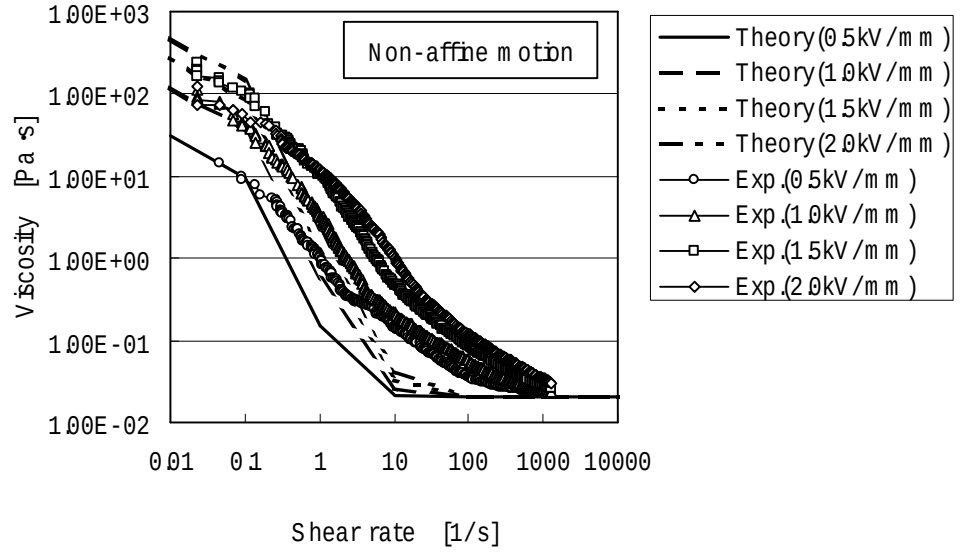

b)

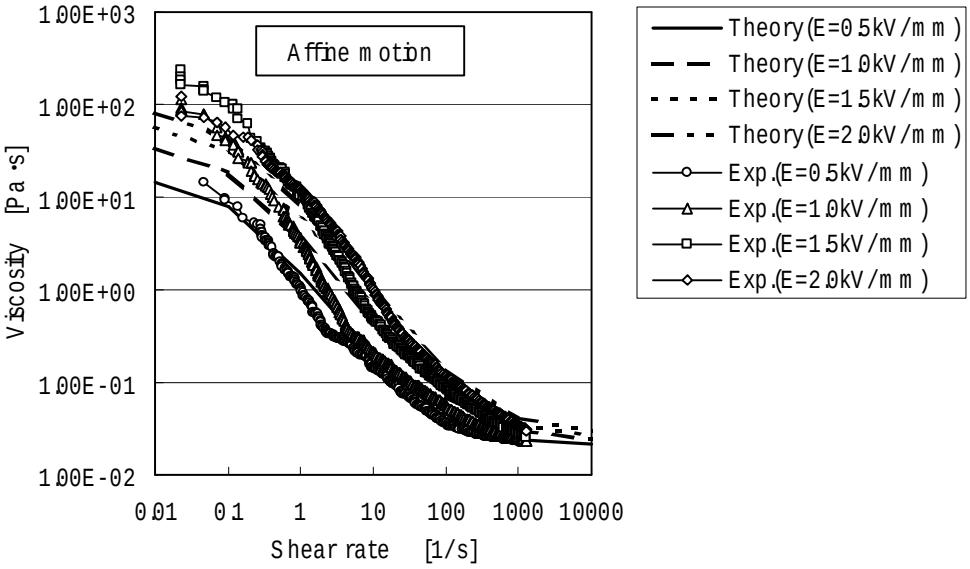

Fig.5. Comparison between experimental data and theoretical results regarding ERF viscosity.

On the other hand, by varying the parameters of M, n_o, μ, b, $\hat{L}$, θ, N, R, and ξ_*, the results of the network theory can be fitted quantitatively to the experimental data for any type of ERF. Therefore, the tendencies of these parameters need to be investigated. In the cases of both affine and non-affine motions,

the viscosity η changing by $\hat{L}, N, M$, and b show the same qualitative tendencies. Therefore, these tendencies are shown only in the case of affine motion as shown in Figs 6a-d. As for θ and R, the viscosity does not change in the cases of both affine and non-affine motions. The main parameter dependent on the creation of the network is $\hat{L}$, and the relation of viscosity and $\hat{L}$ is linear. As the junction number N increases, the viscosity is changed linearly. When the spring constant of a segment increases with the increase of an electric field E, the viscosity is changed largely based on some value of M.

The tendency of viscosity η changing by n_0 and μ differes in the cases of affine and non-affine motions, as shown in Figs 6e-h. At larger n_o and μ, the change of viscosity due to the network's destruction in the case of non-affine motion becomes smaller than that in the case of affine motion. Therefore, as shown by the difference between the velocity of the network and that of the solvent, the viscosity does not change significantly even if the network undergoes a major destruction.

Only in the case of non-affine motion does the viscosity change as a function of slip parameter ξ, as shown in Fig.6i. As the slip between the network and the solvent increases, the level of viscosity decreases.

a)

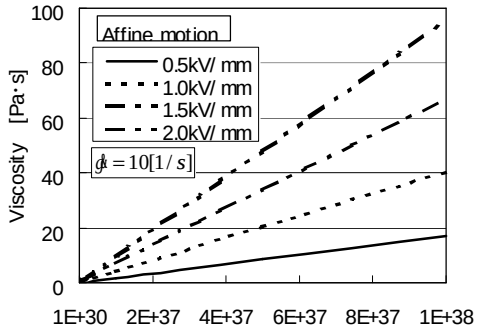

b)

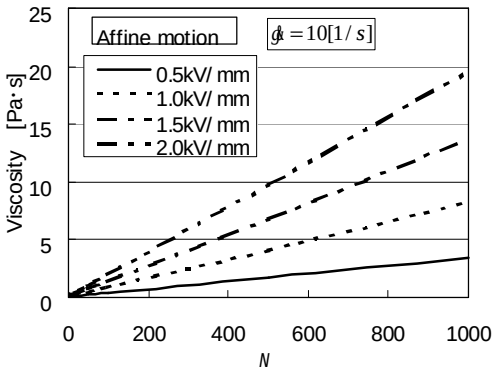

c)

d)

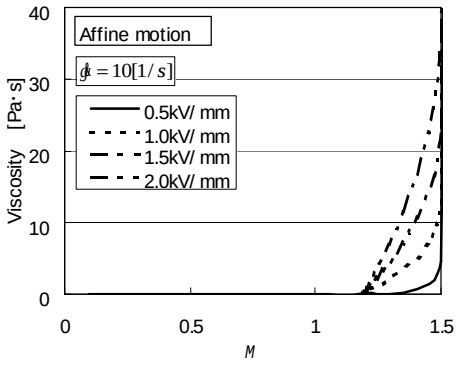
Affine motion
$\dot{\gamma} = 10[1/s]$
0.5kV/ mm
1.0kV/ mm
1.5kV/ mm
2.0kV/ mm
Viscosity [Pa·s]
M

e)

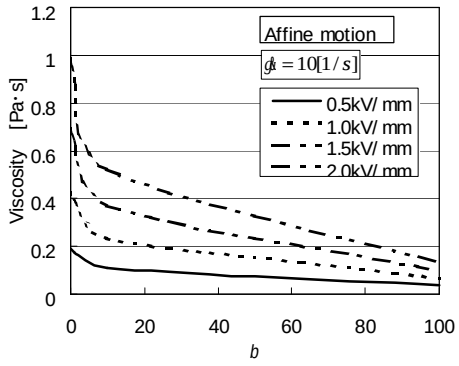
Affine motion
$\dot{\gamma} = 10[1/s]$
0.5kV/ mm
1.0kV/ mm
1.5kV/ mm
2.0kV/ mm
Viscosity [Pa·s]
b

f)

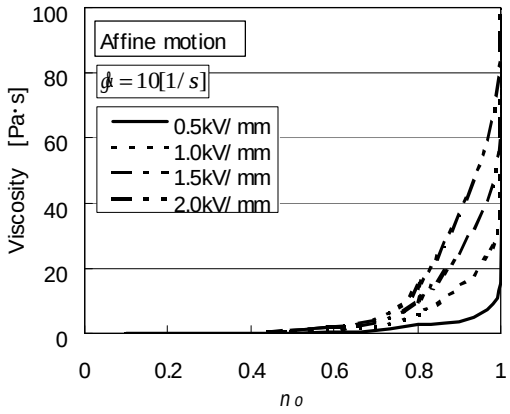
Affine motion
$\dot{\gamma} = 10[1/s]$
0.5kV/ mm
1.0kV/ mm
1.5kV/ mm
2.0kV/ mm
Viscosity [Pa·s]
n_0

g)

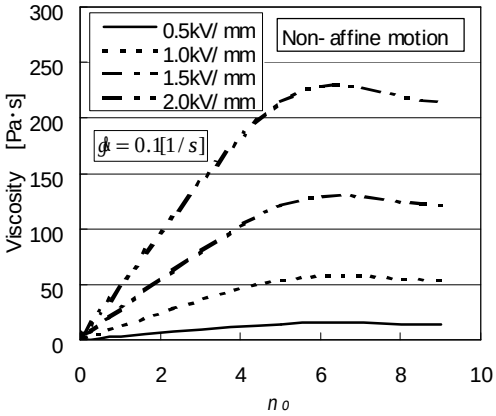
Non- affine motion
$\dot{\gamma} = 0.1[1/s]$
0.5kV/ mm
1.0kV/ mm
1.5kV/ mm
2.0kV/ mm
Viscosity [Pa·s]
n_0

h)

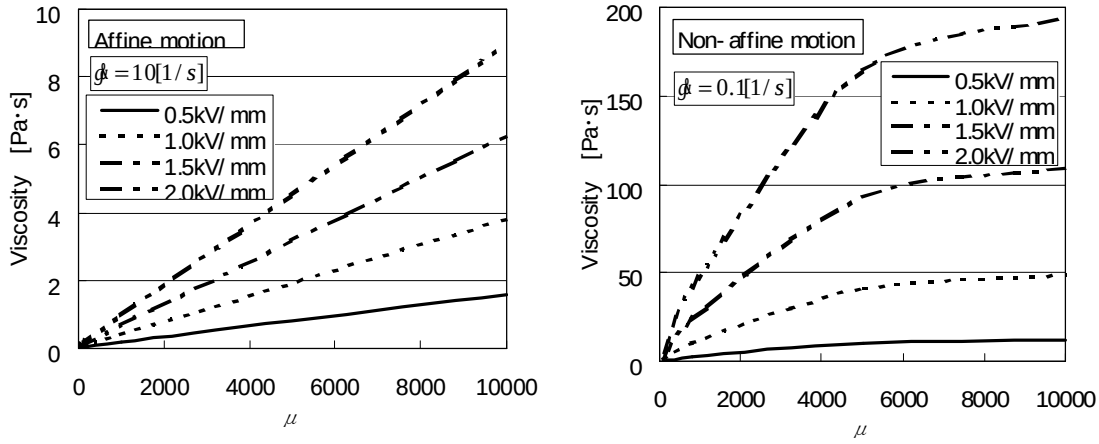

i)

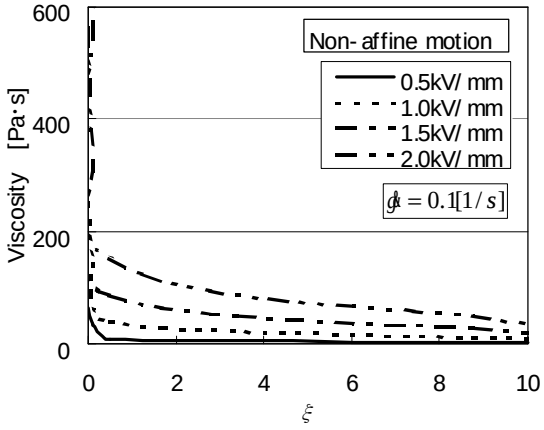

Fig.6. Changing viscosity by parameters in equations of network theory.

By comparison between the results of Figs 5 and 6, in the actual case, it can be guessed that there is no changing of the viscosity by M, ξ, and n_o in the case of affine motion but that there is large changing of the viscosity by b. On the other hand, in the case non-affine motion the changing of viscosity by n_o and μ is larger than in the case of affine motion. The cause is due to the increasing destruction of the network due to larger shear stress.

5. Rectangular duct flow

We compared the theoretical results obtained by the network theory regarding the pressure difference Δp and a given flow velocity v_o in a rectangular duct with the experimental data obtained by Shimada *et al*. (2000d) and Shimada and Kamiyama (2000e). The ERF used in the experiment is the same as that dealt with

in the present network theory. The duct has *15mm* width *w*. The distance between the electrodes *h* is *1.5mm*. The distance between the pressure taps is *150mm*. The pressures are measured in a region when a D. C. electric field is applied.

The theoretical results were obtained by numerical calculation using the results of viscosity of Fig.5. The results of Fig.5 show that the boundary of shear rate between affine motion and non-affine motion was about $0.11/s$ in the numerical calculation. In the calculation, the shear rate of Fig.5 was evaluated as a local shear rate in a duct.

Figure 7 shows the comparison of the present theoretical and experimental results. In addition, the theoretical results obtained by the present network theory and those obtained by considering the ERF as a mechanical dynamic mode are also shown. As for the analytical solution, the equation in the case of a Newtonian fluid in the absence of the electric field was used as shown in Eq.(C1) in **APPENDIX C**, where the viscosity in the absence of the electric field $\eta_{E=0}$ was used. The mechanical dynamic model is a mixture of Maxwell and Voigt models that has been developed by Shimada *et al.* (2000c), as shown in Fig.8.

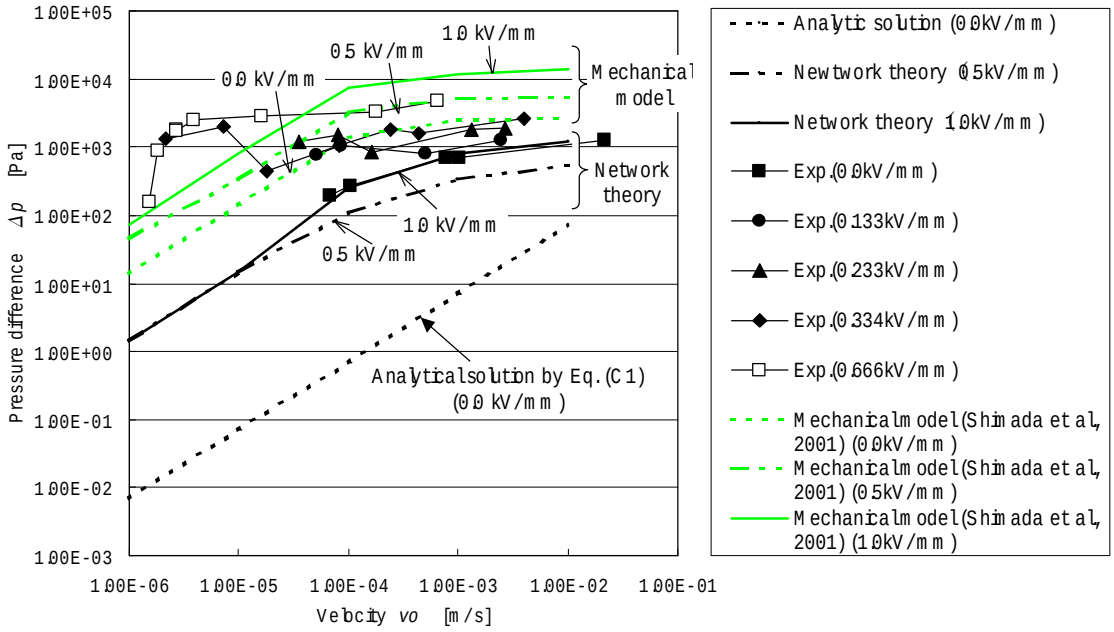

Fig.7. Comparison of theoretical results of network theory to experimental data as well as analytical results and theoretical results of mechanical model.

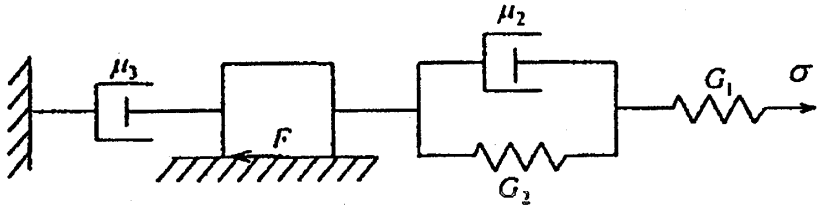

Fig.8. Lamped parameter or mechanisms-based model of ERF by Shimada *et al.* (2000). The model has dashpots with viscosity μ_2 and μ_3, springs with spring constant G_1 and G_2, and friction *F*.

Both under electric and non-electric fields, the experimental qualitative tendency of increasing Δp as increasing v_0 is the same as the tendency in the network theory. In the case of an electric field, at larger v_o, the present network model is close to the experimental data: this range is $\Psi \geq 2\left(v_o \geq 1\times10^{-3}\right)$ on the duct wall. At a large ERF velocity, the particles apparently form a net configuration. At larger ERF velocity, the smectite particles are expanded because more solvent flows between the layers of the particles. The tendency that the length of the smectite particle can change because the smectite particle is elastic, has been investigated by Shimada *et al.* (1996a).

On the other hand, at small v_o range, the results obtained using the network model show a quantitative difference in relation to the experimental data. At this range, the network cannot be created easily. However, at the range that v_o is from 1×10^{-5} to 1×10^{-4}, the mechanical model containing Maxwell and Voigt models by Shimada *et al.* (2000c) can explain the experimental data.

From the above comparison of experimental data to the theoretical results of the network and mechanical models, at the case of rectangular duct, there are both regions of easily creating network and of the particles' correlation without network according to the quantitative amount of flow velocity. However, in the case of the other flow fields, for example, rotating flow, etc., either the network or mechanical models may quantitatively coincide with the experimental data. The subject of the present work is the flow field in the rectangular duct.

6. Conclusions

The following conclusions were obtained regarding a suspension-type ERF based on constitutive equations employing Lodge's network theory, with the theoretical results being compared with the experimental data of viscosity and pressure difference in a rectangular duct.

(1) The decrease in viscosity with an attendant increase in the shear rate can be well explained by using

constitutive equations derived by assuming that the relaxation time λ is a function of the shear rate.

(2) The ratio of viscosity to the shear rate can be explained by the constitutive equation of affine motion in a large shear rate range, and by that of non-affine motion in a small shear rate range. Therefore, the viscosity of ERF can be calculated by using Eq.(2.29) at small shear rate range and Eq.(2.25) at large shear rate range, as refereeing the values of parameters in Fig.6.

(3) The results obtained using the network theory show close quantitative agreement to the experimental results in regard to the pressure difference in a rectangular duct at large flow velocity.

Acknowledgments

This work was partially supported by a grant to RCAST at Doshisya University from the Ministry of Education and Science, Japan.

APPENDIX A

As shown in Fig.1, many junctions in ERF having needle-like whisker particles can be microscopically observed under an electric field. The whisker particle is made of $K_2O_{7.8}TiO_2$ and has a $0.5-0.6\,\mu m$ mean diameter and mean length of $20\,\mu m$. By applying an electric field, the whiskers are aligned along the direction of the electric field line. In the absence of the electric field, the whisker particles are distributed uniformly. The ERF has an ER effect as shown in Fig.2.

APPENDIX B

Figure 3 shows the G' and G'' of ERF containing smectite particles. The G' and G'' are compared with those of polyacrylicamide (PAA) as a normal polymer. In the presence of an electric field, the G' and G'' of ERF are greater than those of PAA. The used PAA is well known to have a network. Therefore, the ERF having smectite particles can be concluded to also have a network.

APPENDIX C

The analytical solution of the pressure difference to flow velocity is given by the following formula

$$\Delta p = v_o \cdot \frac{3\eta_{E=0}}{4h^2\left[1-\frac{192h}{\pi^2 w}\sum_{m=1}^{\infty}\frac{1}{(2m-1)^{2m+1}}\tanh\frac{(2m-1)\pi w}{2h}\right]}. \tag{C1}$$

Nomenclature

a – particle radius $[m]$

b – constant $[1/s]$

E – electric field strength $[V/m]$

$\boldsymbol{F}$ – tension on a segment of the network $[N]$

F – friction force per unit area of slider in the mechanical model $[Pa]$

f – creative ratio of the network per unit time $[-]$

G' – sturage modulus $[Pa]$

G'' – loss modulus $[Pa]$

G_1, G_2 – elastic modulus of spring in the mechanical model $[Pa]$

H – spring constant of a segment between the particles $[N/m]$

H_N – spring constant of a segment between the particles $[N/m]$

k – Boltsmann constant $[J/K]$

L – creative function $\left[1/m^3 \cdot s\right]$

$\hat{L}$ – constant $[1/s]$

M – constant $[-]$

N – number of particles composing the chain $[-]$

n – number density $\left[1/m^3\right]$

n_o – constant $[-]$

P_N – static pressure of network $[Pa]$

P_S – static pressure in the solvent $[Pa]$

$\boldsymbol{Q}$ – end-to-end junction vector for a typical segment of network $[m]$

Q – absolute value of $\boldsymbol{Q}[m]$

$\dot{\boldsymbol{Q}}$ – velocity of end-to-end vector $\boldsymbol{Q}[m/s]$

R – response time from the applied electric field $[s]$

T – absolute temperature $[K]$

t – time $[s]$

$\boldsymbol{v}$ – velocity of solvent $[m/s]$

β – specific permittivity $[-]$

Δp – pressure difference $[Pa]$

$\underset{\approx}{\delta}$ – Kronecker's delta $[-]$

ε_o – permittivity in a vacuum $[F/m]$

$\dot{\gamma}$ – magnitude of the shear rate intensity $[1/s]$

$\underset{\approx}{\dot{\gamma}}$ – shear rate tensor $[1/s]$

η_S – viscosity of the solvent $[Pa \cdot s]$

φ – probability density function $[1/m^3]$

φ_{eq} – probability density function in the quasi-equilibrium state $[1/m^3]$

λ – destruction function $[s]$

μ – constant $[1/s]$

μ_2 . – coefficient of viscosity of dash pot of the Voigt part in the mechanical model $[Pa \cdot s]$

μ_3 – coefficient of viscosity of dash pot in the mechanical model $[Pa \cdot s]$

$\underset{\approx}{p}$ – total shear stress tensor $[Pa]$

$\underset{\approx N}{p}$ – shear stress tensor of network $[Pa]$

$\underset{\approx S}{p}$ – shear stress tensor of solvent $[Pa]$

θ – constant $[m \cdot S/V]$

σ – strain rate $[1/s]$

$\underset{\approx N}{t}$ – shear stress tensor of solvent without $P_N [Pa]$

$\underset{\approx S}{t}$ – shear stress tensor of solvent without $P_S [Pa]$

ξ – slip parameter $[-]$

Ψ – distribution function $[1/m^6]$

ζ – function related to the creation of the network $[m^2/s]$

$\overset{\nabla}{(\text{upper suffix})}$ – upper convective derivative represented

References

ARP P.A., Foister R.T. and Mason S.G. (1980): *Some electrohydrodynamic effects in fluid dispersions.* – Advances in Colloid and Interface Science, vol.12, pp.295-356.

Atkin R.J., Shi X. and Bullough W.A. (1991): *Solutions of the constitutive equations for the flow of an electrorheological fluid in radial configurations.* – Journal of Rheology, vol.35, No.7, pp.1441-1461.

Bird R.B, Curtiss C.F, Armstrong R.C. and Hassager O. (1987): *Dynamics of polymeric liquids, volume2 kinetic theory*. – John Wiley and Sons, Inc. Press, pp.351-391.

Brunn P.O. and Abu-Jdayil B. (1998): *Fluids with transverse isotropy as models for electrorheological fluids*. – ZAMM, Zeitschrift fur Angewandte Mathematik und Mechanik, vol.78, No.2, pp.97-107.

Doi M. (1994): *Electro Responsive Fluids*. – Proceedings of the Japan Society of Mechanical Engineers, No.940-53, pp.219-223 (in Japanese).

Fujita T., Saiki H. and Shimada K. (1997): *Electro-rheological fluid with smectite*. – Report of Smectite, vol.7, No.1, pp.12-20 (in Japanese).

Gamota D.R. and Filisko F.E. (1991): *Dynamic mechanical studies of electrorheological materials: moderate*. – Journal of Rheology, vol.35, No.3, pp.399-425.

Gast A.P. and Zukoski C.F. (1989): *Electrorheological fluids as colloidal suspensions*. – Advances in Colloid and Interface Science, vol.30, pp.153-202.

Gavin H.P., Hansen R.D. and Filisko F.E. (1996): *Electrorheological dampers, Part 1: analysis and design*. – ASME Journal of Applied Mechanics, vol.63, pp.676-682.

Gogosov V.V., Nikiforovich E.I. and Tolmachev V.V. (1979): *Electrization of a low-conductivity liquid flowing through a metal pipe*. – Magnitnaya Gidrodinamica, vol.2, pp.59-62.

Halsey T.C. (1992): *Electrorheological fluids*. – Science, vol.258, pp.761-766.

Huilgol R.R. and Phan-Thien N. (1997): *Fluid mechanics of viscoelasticity*. – Elsevier Science B.V. Press, pp.222.

Johnson A.R., Makin J., Bullough W.A., Firoozian R. and Hosseinisianaki A. (1993): *Fluid durability in a high speed electro-rheological clutch*. – Journal of Intelligent Material and Systems Structures, vol.4, No.4, pp.527-532.

Kamath G.M. and Wereley N.M. (1997): *Nonlinear viscoelastic plastic model for electrorheological fluids*. – Smart Materials and Structures, vol.6, No.3, pp.351-359.

Kim J.W., Kim S.G., Choi H.J., Suh M.S., Shin M.J. and Jhon M.S. (1999): *Synthesis and electrorheological characterization of polyaniline and Na^+-montmorillonite clay nanocomposite*. – Proceedings of 7^{th} International Conference on Electro-rheological Fluids, Magnet-rheological Suspensions, pp.111-118.

Klingenberg D.J., Swol F.V. and Zukoski C.F. (1991): *The small shear rate response of electrorheological suspensions, 1. Simulation in the point-dipole limit*. – Journal of Chemical Physics, vol.94, No.9, pp.6160-6169.

Lee D.Y., Choi Y.T. and Wereley N.M. (2002): *Performance analysis of ER/MR impact damper systems using Herschel-Bulkley model*. – Journal of Intelligent Material Systems and Structures, vol.13, No.7-8, pp.525-531.

Lindler J. and Wereley N.M. (2003): *Quasi-steady Bingham-plastic analysis of an electrorheological flow mode bypass damper with piston bleed*. – Smart Materials and Structures, vol.12, No.3, pp.305-317.

Martin J.E. and Anderson R.A. (1996): *Chain model of electrorheology*. – Journal of Chemical Physics, vol.104, No.12, pp.4814-4827.

Nishida H., Shimada K., Iwabuchi M., Fujita T. and Okui K. (1999a): *Basic characteristics for devices of the rotating concentric cylinder type using ERF with smectite particles*. – Journal of the Japan Hydraulics and Pneumatics, vol.30, No.1, pp.1-9 (in Japanese).

Nishida H., Shimada K., Iwabuchi M., Fujita T. and Okui K. (1999b): *Effects of experimental factors on steady characteristics on devices of rotating disk type using ERF with smectite particles*. – Transactions of the Japan Society of Mechanical Engineers, vol.65, No.629, Ser.C, pp.269-276 (in Japanese).

Nishida H., Shimada K., Iwabuchi M., Fujita T. and Okui K. (1999c): *A study of steady torque characteristics of a rotating disk in ERF (1st report, comparison of flow curve between rotating concentric cylinder and rotating disk.* – Transactions of the Japan Society of Mechanical Engineers, vol.65, No.633, Ser.B, pp.1703-1709 (in Japanese).

Nishida H., Shimada K., Iwabuchi M. and Okui K. (2002d): *Effect of mass concentration and electrode gap on torque characteristics of a rotating disk in ERF*. – Journal of the Japan Hydraulics and Pneumatics, vol.33, No.1, pp.1-8 (in Japanese).

Nishida H. and Shimada K. (2002e): *Characteristics of braking devices using ERF*. – Proceedings of SPIE, vol.4934, pp.340-350.

Oravsky V. (2002): *Quasi-static heat transfer in an experimental device with a radial electro-structured fluid clutch*. – Journal of Intelligent Material and Systems Structures, vol.13, No.4, pp.209-230.

Otsubo Y., Edamura K., Fukube H. and Deyama K. (1997): *Rheological changes of suspensions induced by electrohydrodynamic instability*. – Proceedings of 6th International Conference on Electro-rheological Fluids, Magnet-rheological Suspensions and their Applications, pp.35-42.

Peel D.J., Stanway R. and Bullough W.A. (1996): *A generalized presentation of valve and clutch data for an ER fluid, and practical performance prediction methodology*. – International Journal of Modern Physics B, vol.10, No.23/24, pp.3103-3114.

Prudnikov V.V. (1979): *Instability of a layer of a conducting viscous fluid surrounding a solid rod*. – Magnitnaya Gidrodinamica, vol.4, pp.24-28.

Sasada N. and Honda T. (1980): *Electrorheological effect of fluid and its applications (6)*. – Science of Machine, vol.32, No.6, pp.777-782 (in Japanese).

Shimada K., Fujita T., Iwabuchi M. and Okui K. (1996a): *ER effect in rotating flow of electrorheological fluid with elastic particles*. – Journal of the Japan Society of Powder and Powder Metallurgy, vol.43, No.6, pp.755-770 (in Japanese).

Shimada K. and Fujita T. (2000b): *A device to regulate rotational speed utilizing a rotating regulator with electrorheological fluid*. – Experimental Mechanics, vol.40, No.2, pp.231-240.

Shimada K., Nishida H. and Yamaguchi H. (2000c): *Theoretical analysis of the hydrodynamic characteristics of electrorheological fluid in a parallel duct flow*. – Applied Mechanics and Engineering, vol.5, No.4, pp.803-820.

Shimada K., Nishida H. and Fujita T. (2000d): *Difference in steady characteristics and response time of ERF on rotational flow between rotating disk and concentric cylinder*. – International Journal of Modern Physics B, vol.15, No.6 and 7, pp.1050-1056.

Shimada K. and Kamiyama S. (2000e): *Hydrodynamic characteristics of electrorheological fluid in a parallel duct Flow*. – International Journal of Modern Physics B, vol.15, No.6 and 7, pp.980-987.

Stanway R., Sproston J.L., Prendergast M.J., Case J.R. and Wilne C.E. (1987a): *ER fluids in the squeeze-flow mode: an application to vibration isolation*. – Journal of Electrostatics, vol.28, No.1, pp.167-184.

Stanway R., Sproston J.L. and El-Wahed A.K. (1996b): *Application of electrorheological fluids in vibration control: a survey*. – Smart Materials and Structures, vol.5, No.4, pp.464-482.

Tanaka K., Sahashi A., Akiyama R. and Koyama K. (1995): *Scaling behavior of response times of electrorheological suspensions with chain exchange resin particles*. – Physical Review, vol.52, No.4, pp.R3325-R3328.

Wereley N.M. and Pang Li (1998): *Nondimensional analysis of semi-active electrorheological and magnetorheological dampers using approximate parallel plates models*. – Smart Materials and Structures, vol.7, No.5, pp.732-743.

Whittle M., Atkin R.J. and Bullough W.A. (1995): *Fluid dynamic limitations on the performance of an electrorhelogical clutch*. – Journal of Non-Newtonian Fluid Mechanics, vol.57, No.1, pp.61-81.

Yang F. (1997): *Tension and compression of electrorheological fluid*. – Journal of Colloid Interface Science, vol.192, pp.162-165.

Zkakin A.I. and Tarapov I.E. (1979): *Electrohydrodynamical instability of a weakly conducting fluid between two cylindrical electrodes with unipolar injection*. – Magnitnaya Gidrodinamica, vol.4, pp.53-57.

Received: June 4, 2004

Revised: March 29, 2005